Utrecht University

Master Thesis (30 EC)

Determinants of the distribution of plant-functional traits

Relationships with climate and fire across spatial gradients in Australia

Samuel. A. Tofts

October 23, 2020

Solis-ID: 6485812
Sustainable Development MSc
Track – Environmental Change and Ecosystems
Faculty of Geosciences, Utrecht University
s.a.tofts@students.uu.nl

Supervisor: Dr. Mara Baudena (Utrecht University)
External Contributor: Professor. Sandy Harrison (University of Reading)

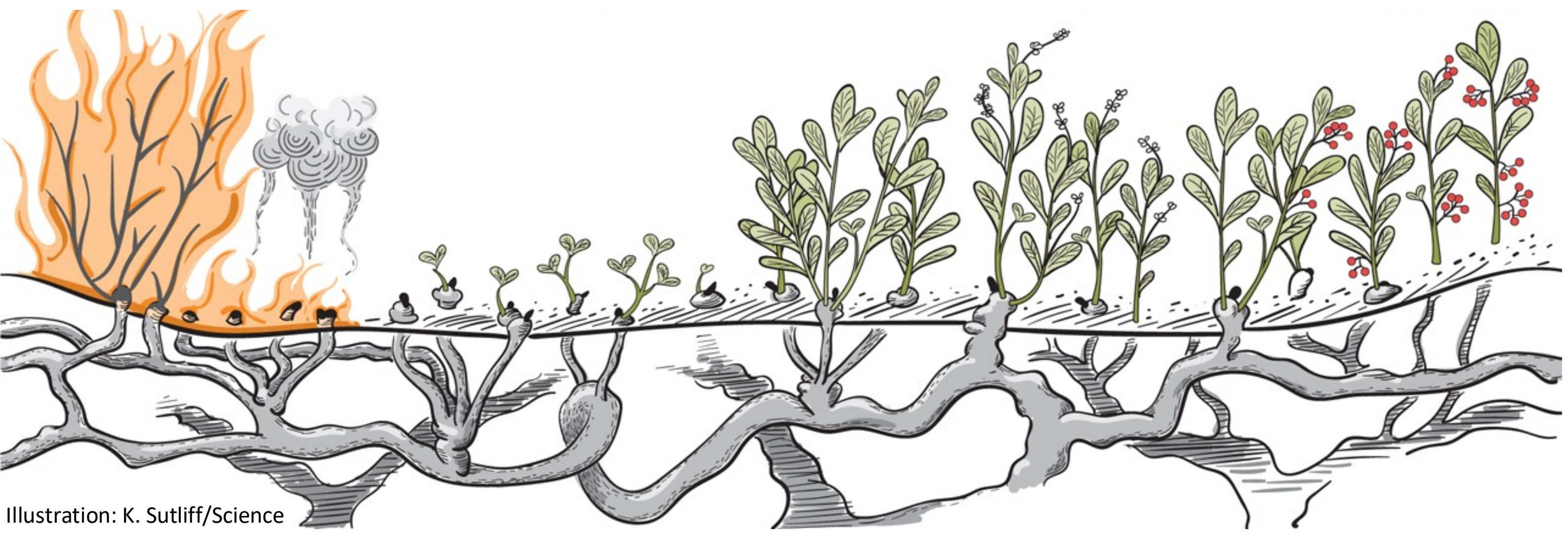

Illustration: K. Sutliff/Science

Summary

Fire-prone ecosystems are comprised of vegetation with a range of functional traits that confer persistence post-disturbance. Resprouting denotes the functional trait in plants that enables vegetative regeneration after said disturbance events via bud banks located in a range of parts of the plant. In order to do identify the relationships with resprouters and abiotic variables, vegetation data collected from plots located in four areas of Australia was analysed using generalized linear models using climate and fire data as predictor variables. Vegetation variables included relative resprouter richness and percentage of resprouters based on bud bank location: apical (aerial), epicormic (aerial), basal/collar and underground. The results indicated that relative resprouter richness was influenced by increasing mean annual rainfall and decreasing average fire interval. Mean annual rainfall and rainfall seasonality also played a role in determining the prevalence of the various resprouting functional traits. The quantified relationships provide a means of assessing vegetation dynamics and fire regimes in future modelling studies.

Contents

1 Introduction

Disturbance events describe the temporary loss of life within an ecosystem as a result of large-scale perturbations that significantly alter community compositions. Disturbance-prone ecosystems are populated by vegetation evolved with functional traits that enable community persistence throughout multiple disturbance events as is the case for fire-prone (Clarke et al. 2013) and drought-prone (Bred & Badeau, 2008) ecosystems. The distribution and composition of these plant communities are governed by a range of feedbacks within and between the environment and vegetation. Changes to these ecosystem dynamics therefore results in variation in the scale and frequency of disturbance events such as fire (Westerling et al. 2011; Adams, 2013). The resulting feedback effects are able to alter the successional trajectory of an ecosystem giving rise to alternative stable states that are self-reinforcing (Baudena et al. 2020; Adams, 2013; Lasslop et al. 2016).

Fire regimes are a fundamental physiochemical process that influences spatial distribution and composition of vegetated ecosystems (Lasslop et al. 2016; Staver, et al. 2011). The dynamic nature of fires results in fluctuations on the carbon cycle (Yue et al. 2016) and surface albedo (Williams et al. 2012) at a global scale. Fire regimes have fluctuated in a range of natural variability for millennia (Marlon et al. 2008) as a consequence of temporal variations in meteorological variables such as wind, rainfall, air temperature, relative humidity and solar radiation (Williams et a. 2012). The "intermediate-fire productivity hypotheses" (Pausas & Bradstock, 2007; Keeley et al. 2011; Pausas & Ribeiro, 2013) is a widely accepted theory (Karavani et al. 2018) stating that fire activity is highest at intermediate levels of productivity and aridity as a result of a trade-off of the two which determine fuel availability and drought respectively. In this sense, climate change would have differing effects to fire regimes of different ecosystems (Pausas & Ribeiro, 2013).

Fire-prone ecosystems accommodate vegetation with a range of functional traits adapted to facilitate post-fire recovery. Traits include obligate seeders that rely on post-fire recovery by means of recolonization through sexual reproduction post-disturbance. Fire-resistance confers the observed traits that provide a low flammability effect, allowing survival to the individual via adaptations such as thick bark and insulated regenerative material to protect internal systems from fire damage (Williams et al. 2012). Resprouting denotes the ability of a plant to develop, sustain and protect a viable bud bank that enables vegetative regeneration from previously burned individuals whose autotrophic capacity may have been completely destroyed. The resprouting trait is present in a wide range of angiosperms, particularly in arboreal *Eucalyptus* of Australia, the trait is also present, if not less common in gymnosperms such as *Podocarpus* (Keeley et al. 2005).

The resprouting trait is displayed in a wide variety of species and consequently has a number of types based on the production and preservation of meristematic tissue in the form of buds or budforming tissue (Clarke et al. 2013). Presence of these buds at various parts of the plant gives rise to the broad classification of aerial, basal or below-ground resprouters. There is however variation within these classes based on how these bud banks are protected, number of buds and the location of non-structural carbohydrates used as storage reserves. Based on this Clarke et al. 2013 identified four main resprouting types: apical (aerial resprouters that protect the apex bud), epicormic (aerial resprouters where shoots originate from the bole and branchlets), basal (buds located at ground level) and below-ground (bud banks are stored underground). Prominence of the various functional traits naturally depends on a range of variables (Figure 1) including the frequency and nature of disturbance events as well as bioclimatic variables, all of which presents interactions with one another.

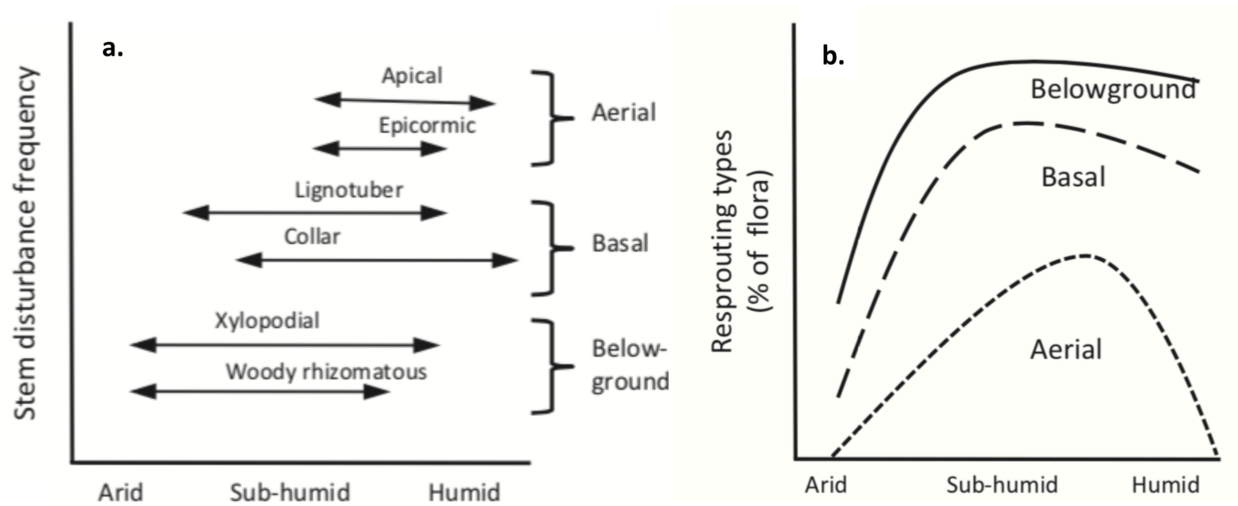

Figure 1. Conceptual relationships between resprouter types, rainfall gradients and **a)** stem disturbance frequency an **b)** relative proportion of functional trait in a community. Adapted from Clarke et al. 2013

The vegetation in turn play a role in determining fire characteristics, generating further feedback (Archibald et al. 2013). Generally, communities dominated by resprouters have been shown to recover from disturbance more quickly than those where resprouters are absent (Zeppel et al. 2014). Conversely, obligate seeders are typically favoured in areas where disturbance events are less common (Russel-Smith et al. 2012). Given projected climate change and changing fire regimes, there is potential for shifts in the distribution of fire adapted vegetation (Enright et al .2014; Baudena et al. 2020).

Australia is known as one of the most fire-prone countries globally, with at least one area part of the country experiencing a form of fire season at any one time (Williams et al. 2012). Regarding fire season, five broad fire seasons have been classified by Luke & McArthur (1978) based on fuel dryness, availability and likelihood of ignition and spread. Fire season in the North begins in winter/spring, moving down throughout the year and afflicting the south by summer/autumn. In the most recent 2019-2020 wildfires, >12 million hectares area including forest and agricultural lands were burned, this has mainly been attributed to a prolonged drought and record-breaking high temperatures (Boer, de Dios & Bradstock, 2020). Monetary costs alone in damage caused by the fires is set to exceed the A$4.4 billion in costs of the 2009 "Black Saturday" fires, (Ell, 2020) the series of fires which were among Australia's worst and most costly (Ell, 2020). These costs are expected to increase in terms of damage to other economic activities such as tourism. Furthermore, damage to ecosystem services such as nutrient cycling and carbon storage, loss of biodiversity and shifting community assemblages, are a number of ecological consequences of increasing wildfires. Evidence of significant reductions in post-fire tree regeneration within the 21st century in US Rocky Mountains (Stevens-Rumann et al. 2018) and *Eucalypt* forests in south-western Australia (Etchells et al. 2020), necessitates the fact that fire-adapted ecosystems have limitations concerning recovery. Regarding the suite of feedbacks that occur within fire prone ecosystems, there is potential for this to alter successional trajectory of communities, changing the community compositions (Enright et al. 2014; Adams, 2013) In order to predict and mitigate emerging fire patterns, better understanding needs to be gained on the relationships that vegetation has with fire and climate at a landscape-scale.

Faced with the uncertainty regarding future climate and its implications to future fire regimes (Moritz et al. 2012), there is a growing necessity for models whose statistical relationships reflect underlying processes (Bistinas et al. 2014). This can be highlighted by the disagreement at both global and regional scales in previous modelling studies (Bistinas et al. 2014; Moritz et al. 2012) even under the same emissions scenarios. An understanding of the interactions that underly fire regimes require a large degree of testing, data contributions and real-world comparisons in order to develop adaptive management policies and measures that promote natural, manageable fire regimes. In order for these to be implemented, a better understanding of what drives post-fire responses of vegetation is needed.

Despite the activity in the study of resprouting and the implications of their presence in a community, quantitative data regarding the relationships between environmental variables and the distribution and expression of resprouting traits remains poor for many regions. Thus, understanding of the feedbacks that govern fire prone ecosystems are somewhat limited. As a consequence of this, only a small number of studies have included resprouters in modelling studies (Kelley et al. 2014; Baudena et al. 2020) and subsequently climate projections (Kelley & Harrison, 2014). In order to make accurate projections for Australian ecosystems that includes post-fire recovery, the relationships between environmental variables and distribution of resprouting vegetation needs to be better understood.

A great deal of data already exists on post fire responses of vegetation in Australia (Russel-Smith et al. 2012; Enright et al. 2011; Bradstock & Kenny, 2003), as does fire and climate data. What is less known is the precise factors that determine post-fire responses over large temporal and spatial scales. Retrospective studies provide a means of analysing past data in order to determine the main determinants of resprouter distributions. This study aims to develop empirical relationships between environmental variables and the distribution of functional traits that confer post-fire recovery within a number of fire-prone ecosystems of Australia, answering the following research questions:

Main research question:

What is the relationship between the distribution of resprouting vegetation with fire regimes and climate across different Australian ecosystems?

Sub-questions:

SQ.1 What are the main determinants of the prevalence of resprouting taxa within plant communities?

SQ.2 What are the main determinants of resprouter type occurrence within plant communities? How do the identified relationships for resprouter types differ from each other?

Regarding the above research questions, the following hypotheses have been formulated:

H.1 There will be a strong, negative correlation between average fire interval and percentage of resprouters relative to all vegetation.

H.2 Percentage of resprouter species will peak at intermediate levels of rainfall.

H.3 Rainfall and fire frequency will be the main determinants of resprouter type.

H.4 Spatial distribution of resprouters will be heavily associated with bioclimatic variables that are linked to fire regimes.

1.1 Theoretical Design

Analysis of the spatial distribution of vegetation relative to environmental gradients underlies ecological research. Statistical modelling such as generalized linear models (GLMs), enables the quantification of these relationships, providing insight into the effects of environmental variation on plant communities. GLMs rely on assumed relationships between independent variables and dependant variables of a range of distribution-types, enabling non-linear relationships to be derived (Guisan, Edwards & Hastie, 2002). Within ecology this does not provide objectivity, but, as defined by Burnham & Anderson (2002), an “approximation of the explainable information in the empirical data, in the context of the data being a sample from some well-defined population or process”. Due to the complex nature of ecosystems and the array of interacting biotic and abiotic variables, overfitting of variables to models is regarded as a common issue that results in issues with inference (Burnham & Anderson ,2002). Further issues arise from the relationships between predictor variables, if one influences another, then deduction of their relationships with the response variable becomes an issue. As a result of the underlying issues, simplicity is a desired characteristic in models with focus given to fewer, uncorrelated predictor variables that best explain the response variable. This leads to the process of model selection, the identification of the most holistic yet least overfitted model. In the present study, Akaike’s Information Criterion (AIC) was used as an evaluative metric that estimates the distance or information lost when using any one model compared to that of the true defining mechanism, represented by the log-likelihood function at its maximum point. This theoretical distance does, however, increase with the addition of parameters as a consequence of the added “noise”. Lower AIC values therefore represent the models closeness to “reality”, models are however ranked relative to the set rather than the absolute AIC value (Akaike, 1974; Burnham & Anderson, 2002).

3 Methodology

3.1 Study Sites

The study focuses on four regions of Australia: northern Australia, southwestern Australia, the Sydney Basin and southern New South Wales (Figure 2). The northern Australia sites (Figure 2a) climate is characterised as seasonal summer-wet. Plot data was obtained in *Eucalyptus* savanna woodlands and sandstone heaths of three national parks (Kakadu, Litchfield and Nitmiluk) located in the high rainfall zone (>1000 mm per year). The southwestern Australia site, (Figure 2b), with a seasonal winter-wet climate is dominated by *Eucalyptus* & *Corymbia* forest in the southern-most part of studied area with *Banksia* woodland in intermediate sites and shrublands in the northern sites. The Sydney Basin and southern New South Wales (Figure 2c) climates are described as non-seasonal and are occupied by coastal and hinterland mountain regions respectively. The predominant vegetation in these areas is open forest & woodland, often with a shrubby understory and with patches of heaths, shrublands and rainforest occurring throughout.

3.2 Data Description

Due to the nature of the vegetation data collection in that it spanned a number of years, climate and fire data was collected for the maximum number of years in which all types of environmental data was available in order to form a shared climatology for 1997-1999. The argument for this is that the predominantly woody resprouting woody species are reflective of a number of years of environmental influence. Furthermore, large regional differences in climates can still be represented.

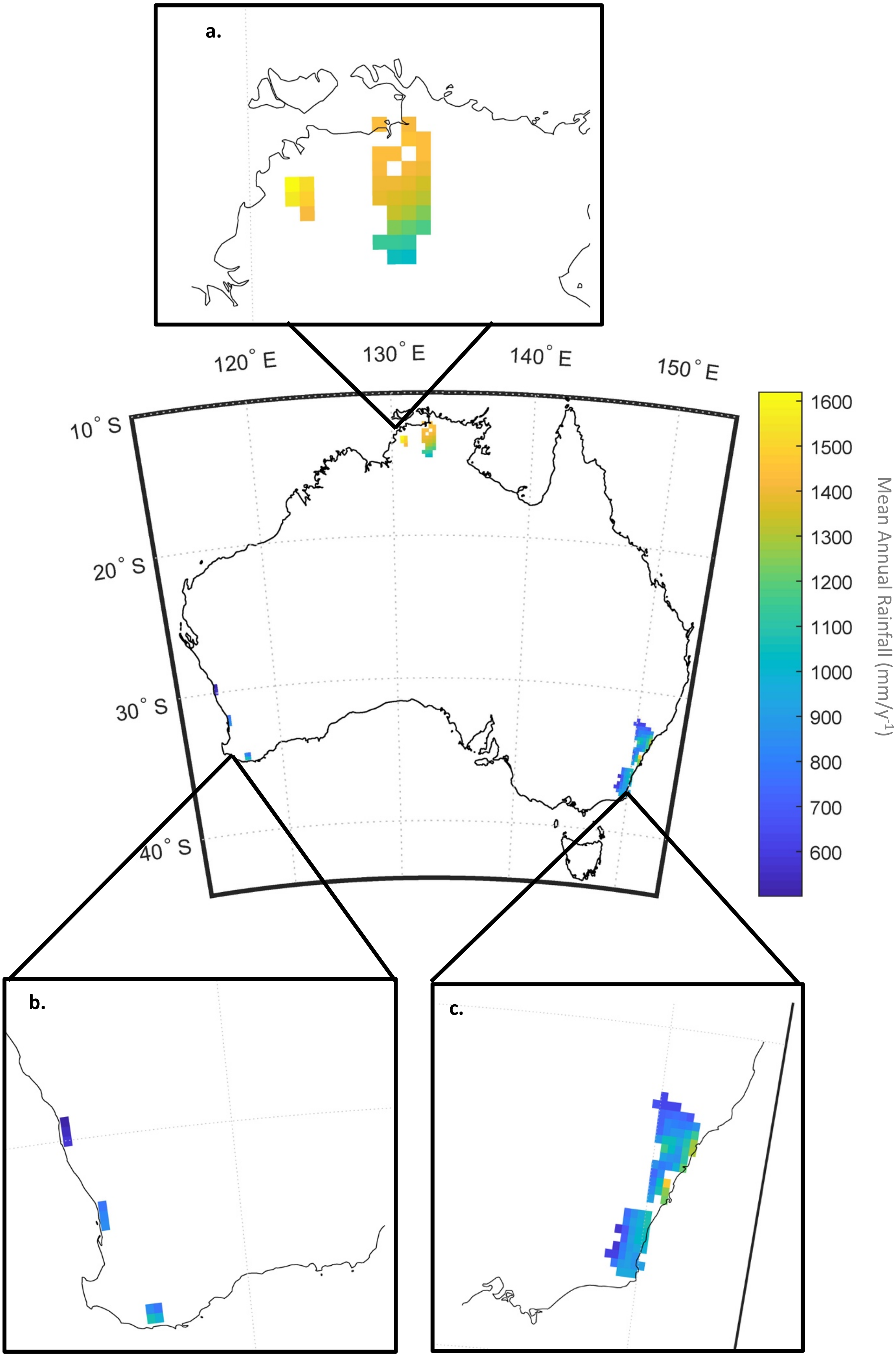

Figure 2. Australia gridded to 0.25° grid cells, coloured cells indicate cells in which sites are located; colour scale indicates mean annual rainfall of years 1997-1999 (mm/year^{-1}). Sites of vegetation collection are **a)** northern site **b)** southwestern site **c)** Sydney basin & southern New South Wales

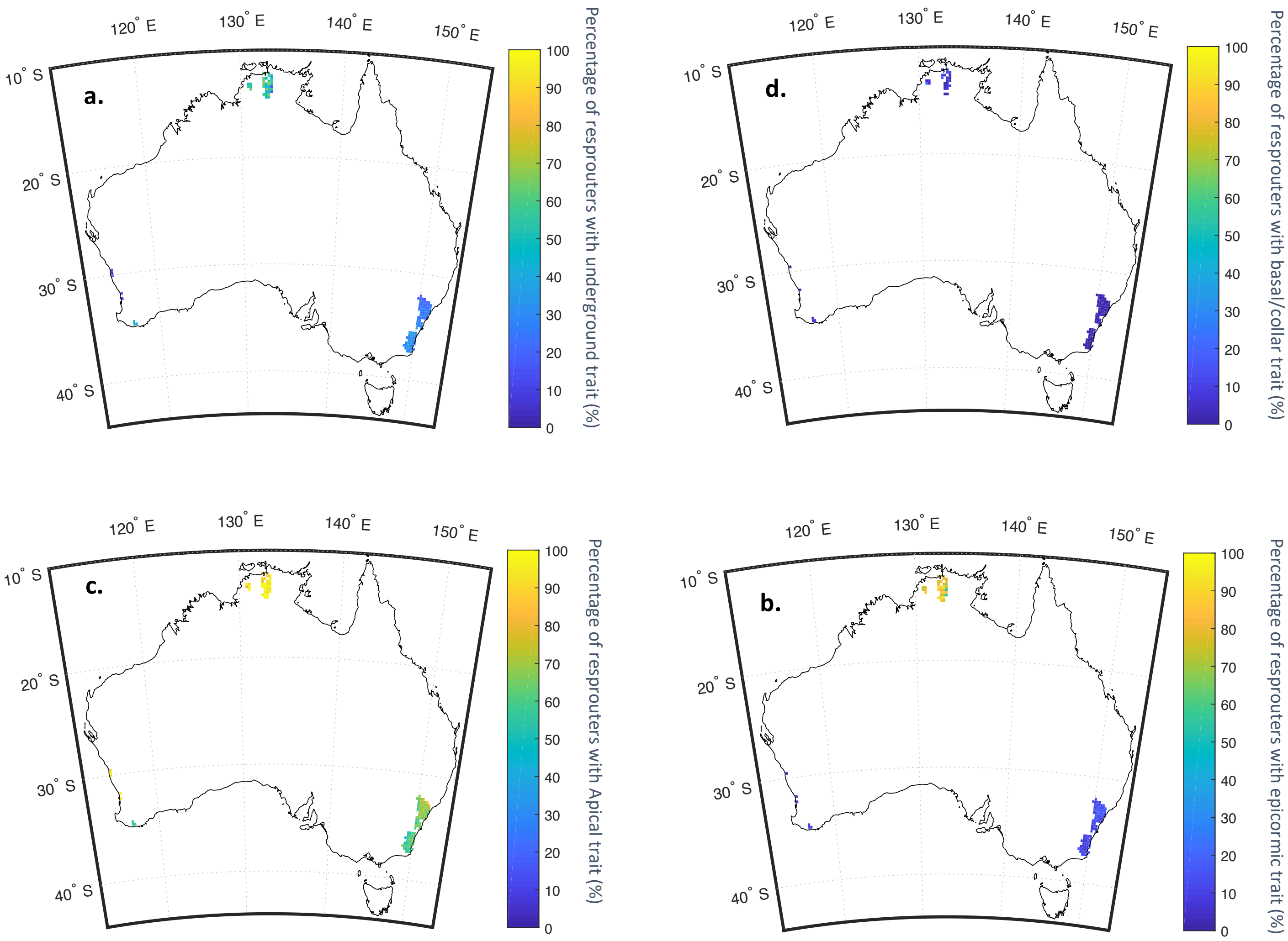

Figure 3. Site maps of Australia showing percentage of resprouting plants exhibiting the **a)** underground **b)** epicormic **c)** apical and **d)** basal/collar resprouting traits

3.2.1 Vegetation

All vegetation data was previously collected in a combination of separate studies. At the northern sites (Edwards et al. 2003), vegetation sampling was conducted from 1995 finishing in 2000. The south-western site data (Enright et al. 2011; Pekin et al. 2011) was collected in spring 2007-2009. The south-eastern site, including the Sydney Basin and southern New South Wales was collected in a series of studies, amassed by Bradstock & Kenny (2003). Data was compiled and kindly provided by Professor Sandy Harrison, Reading University). The vegetation data is therefore collected over a number of years and with a range of sampling techniques described below.

In the northern sites, the basal area of live adult trees diameter at breast height (DBH) ≥ 5cm was assessed in 20 × 40 m plots. The densities of small woody understorey plants (<50 cm height) including juvenile trees and true shrubs were assessed in two 40 × 1 m transects within each tree plot. The densities of medium (0.5—2 m height) and large (>2 m height) woody understorey plants were assessed in one 40 × 10 m sub-plot within each tree plot. A total of 137 and 20 plots were made for the savanna woodland and sandstone heath plots respectively. In the southwestern sites all vascular plants were measured within 10 x 10m plots in the northern sites and 30 x 30m plots in the southern forest during Spring 2007-2009. In the Sydney Basin and southern New South Wales sites cover abundance scores for all vascular plants was collected from 0.1 ha plots.

Species abundance data was collected for each site with each species being classed as either a non-resprouter, seeder (soil or aerial) or resprouter (apical, epicormic, basal/collar & underground) according to Clarke et al. 2013. Due to the varying methodology of the vegetation data collection, percentage cover for species were estimated and abundance scores calculated to allow comparison. This was done by taking the mid-point of Braun-Blanquet percentage ranges that had been used to calculate abundance for the southwestern sites.

For sites where Braun-Blanquet percentage ranges had not been taken, a simple linear relationship between basal area of vegetation and cover was used to estimate percentage cover. All percentage covers were then converted to Braun-Blanquet scores so abundance could be derived (Table 1). For plots where individual size classes were counted, total cover was estimated using allometric relationships between individual heights and cover. Percentage cover was then converted to Braun-Blanquet values to calculate abundance scores.

Table 1. Braun-Blanquet cover abundance scale conversion to midpoint range cover

Braun-Blanquet Scale	*Range of Cover (%)*	*Midpoint of Range Cover (%)*
5	75-100	87.5
4	50-75	62.5
3	25-75	37.5
2	5-25	15
1	<5 numerous individuals	2.5
+	<5 few individuals	0.1

3.2.2 Climate Data

Mean annual temperature (MAT) and mean annual rainfall (MAR) were derived from monthly rainfall and temperature, obtained at 0.05° resolution from the TERN AusCover, Australian Gridded Climate Dataset (Tern AusCover, 2020) covering the years 1997-1999. Data was upscaled to 0.25° resolution in order for comparison with other data sets and to allow for a coarser overview of variables.

Monthly rainfall and temperature data was then used to derive precipitation during the month of maximum rainfall (Pwet), precipitation during month of minimum rainfall (Pdry), temperature during month of maximum rainfall (Twet) and temperature during month of minimum rainfall (Tdry). Dry Months (DM) were calculated as months in which rainfall was below 5mm/d^{-1}. All variables were calculated individually by year and then averaged (mean) over the 4 years in order to form a climatology.

Average rainfall seasonality index (SI) describes the variability of monthly rainfall throughout the year and was derived from monthly rainfall data based on Walsh & Lawler (1981). The SI ranges from 0 (indicating equal distribution of rainfall throughout the year) to 1.83 (indicating total yearly rainfall occurs in one year). Monthly rainfall measurement from 1997-1999 were used to produce the rainfall seasonality index (SI). In order to quantify the index the sum of the absolute deviations of mean monthly rainfall ($\overline{x}_n$) from the mean annual rainfall per year ($\overline{R}$) summarized as:

$$SI = \frac{1}{\overline{\overline{R}}} \sum_{n=1}^{n=12} \left| \, \overline{x}_n - \overline{R}/12 \right|$$

Growing Days (GD), defined as days in which temperatures exceeded 10^{o}C and potential evapotranspiration (PET) data was obtained at 0.01^{o} resolution from the eMAST-R-Package collection (Xu et al. 2015). Data was then upscaled to 0.25^{o} resolution in order to fit into the aforementioned climatology.

3.2.3 Fire Data

Monthly burned area data (BA) was obtained at 0.25^{o} resolution from the Global Fire Emissions Database (GFED4) (Giglio, Randerson & van de Werf, 2013). Data spanned from 1997-1999, from this a monthly mean was formed for each 0.25^{o} cell. Months of burn (MOB) was calculated by summing the months in which the burned area fraction was >1%, this was then averaged across the years to form a single unit per 0.25^{o} cell. Average fire interval (AFI) was then calculated by means of inverting the annual average burned area fraction:

$$AFI = \frac{1}{BA}$$

Infinity values were avoided by means of converting any infinity AFI values to 9999.9 years which was therefore the maximum AFI value. Due to issues regarding the magnitude of AFI, the $\log_{10}$AFI was subsequently used in all data analysis (D'onofrio et al. 2018).

Fire radiative power (FRP) data was obtained from the moderate resolution imaging spectroradiometer (MODIS 6) collection (MODIS 6 Collection, 2020).

Fire seasonal concentration (FSC) describes the variability and spread of fire throughout a year through means of a vector between 0-1, a value of 1 indicating yearly fire concentrated within a single month, 0 being equally distributed throughout the year. FSC was calculated according to Kelley et al. (2012),

For each month (*t*), a vector was formed, the length of which corresponds to the magnitude of BA, with the direction (θ_t) corresponding to month *t*. January is thus set to an angle of zero.

$$\theta_t = 2\pi(t-1)/12$$

Following on from this, a mean vector *L* was calculated through averaging of the real and imaginary parts of the 12 vectors (x_t):

$$L_x = \sum_t x_t \cos(\theta_t) \quad \& \quad L_y = \sum_t x_t \sin(\theta_t)$$

The FSC is then formulated by dividing the length of the mean vector by the annual value:

$$FSC = \frac{\sqrt{L_x^2 + L_y^2}}{\sum_t x_t}$$

Table 2. Vegetation, fire and bioclimatic variables, units and definitions

Variable	*Abbreviation*
Percentage of Species with Resprouting Trait (%)	RSpPer
Percentage of Resprouters with Apical Trait (%)	Apical
Percentage of Resprouters with Epicormic Trait (%)	Epicormic
Percentage of Resprouters with Basal/Collar Trait (%)	Basal/Collar
Percentage of Resprouters with Underground Trait (%)	Underground
Logarithmic Average Fire Interval	Log^{10}AFI
Months of Burn	MOB
Fire Radiative Power	FRP
Fire Seasonal Concentration	FSC
Mean annual rainfall (mm/y^{-1})	MAR
Precipitation during the month of maximum rainfall (mm)	Pwet
Precipitation during the month of minimum rainfall (mm)	Pdry
Temperature during the month of maximum rainfall (°C)	Twet
Temperature during the month of minimum rainfall (°C)	Tdry
Average rainfall seasonality index	SI
Dry Months	DM
Growing Days ($d^{-}1$)	GD
Potential Evapotranspiration ($mm/month^{-1}$)	PET

3.3 Data Analysis

Vegetation data was averaged within each cell to produce mean values for resprouter species richness relative to total species richness (RSpPer(%)). Vegetation had been classed by resprouter traits: apical, epicormic, basal/collar and underground. It should be noted that in some cases, resprouting vegetation was not able to be properly classified to the species level in the field and therefore has no functional trait listed other than resprouter or non-resprouter. Conversely, species exhibiting multiple resprouting traits are therefore represented in multiple categories of functional trait. Percentage of resprouting plants with each subsequent trait was then calculated. Data was then averaged (mean) into each 0.25° cell to provide an average. Due to the spatially uneven sampling nature of the data, focus was given to the proportions of taxa relative to the total number of taxa (Russel-Smith et al. 2012). When focusing on specific resprouting traits, these were expressed as proportional values of general resprouting taxa.

In order to assess collinearity between input variables beforehand, *r* values (Pearson's Correlation Coefficients) were calculated between each variable (Table 2). A threshold value of correlation coefficients was set at >0.7, in which variables were either exempted from the GLMs or not used together in the same GLM (Booth, 1994; Dormann et al. 2013). Relationships between climate, fire and vegetation data was analysed using generalized linear models (GLMs). Independent variables were fitted with a binomial distribution using a logit function. All predictor variables were standardized through subtraction of the mean and dividing by the standard deviation so as each variables coefficient magnitude was representative of its significance in the model by means of being on the same scale (D'Onofrio et al. 2019). Variables were included individually up to the third order and in various combinations. Model selection was based on the Akaike information criterion (AIC), which was used to calculate the ΔAIC, defined as the difference between the AIC of any one model and the value of the model with the lowest AIC score (Akaike, 1972; Burnham & Anderson, 2002; D'Onofrio et al. 2019). Goodness of fit was determined by means of the explained deviance (pseudo-R^2, hereby referred to as R^2) the equivalent to explained variance in least squared models (Guisan & Zimmermann, 2000).

All data analysis was carried out using Matlab R2017a, models were fit using the Matlab function 'fitglm' and Pearson's correlation coefficients generated using 'corrplot'.

4 Results

As a result of the collinearity assessment, a number of variables were exempted from use in the GLMs, due to high degrees of collinearity with other variables (Appendix 1). Variables that were used in the GLMs (Table 3) that showed a Pearson's correlation coefficient of >0.7 e.g. SI & MAR, were not used in the same GLM.

Table 3. Pearson's r coefficients between independent variables: Mean annual rainfall (MAR), precipitation in the driest month (PDry), temperature in the driest month (TDry), dry months (DM), seasonality index (SI), potential evapotranspiration (PET), growing days (GD), log^{10} average fire interval, months of burn (MOB), fires seasonal concentration (FSC). Bold numbers indicate r values that were >0.7

	MAR	***PDry***	***TDry***	***DM***	***SI***	***PET***	***GD***	***Log^{10} AFI***	***MOB***	***FSC***
MAR	**1.00**									
PDM	-0.39	**1.00**								
TDM	0.58	**-0.88**	**1.00**							
DM	**0.73**	**-0.82**	**0.85**	**1.00**						
SI	**0.71**	**-0.87**	**0.89**	**0.96**	**1.00**					
PET	0.47	**-0.78**	**0.76**	**0.80**	**0.79**	**1.00**				
GD	0.69	**-0.84**	**0.89**	**0.93**	**0.93**	**0.93**	**1.00**			
Log^{10} AFI	-0.65	0.59	**-0.71**	**-0.75**	**-0.74**	-0.65	**-0.79**	**1.00**		
MOB	0.50	-0.11	0.18	0.40	0.30	0.31	0.41	-0.56	**1.00**	
FSC	0.16	0.30	-0.28	-0.06	-0.17	-0.07	-0.04	-0.25	0.39	**1.00**

4.1 Resprouter Species Percentage

The main determinant in the acceptable models (Table 4) was MAR, with MAR alone proving to be the best model (R^2 = 0.34) based on its relative AIC value. Inclusion of other variables resulted in reduced R^2 values in all but one of the models. Addition of log_{10}AFI improved the explained deviance by 0.059 at the cost of a higher relative AIC value (Figure 4). A full list of the GLMs can be found in Appendix 2.

Table 4. Best GLMs (ΔAIC < 2) for resprouter species percentage (RSpPer) and resprouter percentage cover (RPer). Predictors are MAR, logarithmic average fire interval (log10(AFI)), rain seasonality index (SI), dry months (DM), potential evapotranspiration (PE) and temperature in the driest month (TDryMonth)

Response variable: Resprouter Species Percentage		
Best model	***R^2***	***ΔAIC***
Logit(RSpPer) = 1.403 + 0.437 MAR	0.34	0.00
Logit(RSpPer) = 1.376 - 0.307 log_{10}AFI	0.18	1.67
Logit(RSpPer) = 1.378 + 0.320 SI	0.18	1.73
Logit(RSpPer) = 1.376 + 0.308 DM	0.16	1.93
Logit(RSpPer) = 1.405 + 0.390 MAR - 0.074 log_{10}	0.40	1.93
Logit(RSpPer) = 1.443 + 0.442 MAR - 0.042 MAR^2	0.34	1.96
Logit(RSpPer) = 1.403 + 0.442 MAR - 0.014 PE	0.39	2.00

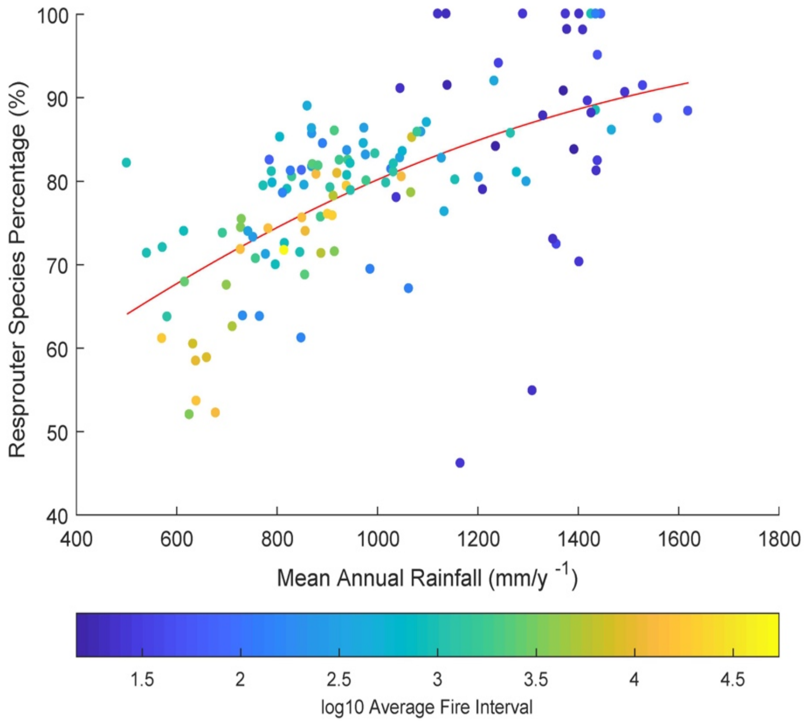

Figure 4. Resprouter species (%) as a function of mean annual rainfall (mm/year^{-1}). Continuous line is the best fit model between resprouter species and MAR. Colors indicate the log^{10} average fire interval, warmer colors indicate longer average fire intervals

4.2 Resprouting Traits

Due to extremely high explained deviance values, and the fact that all the best GLMs for all traits had only log^{10}AFI at an AIC low enough for all other variables to be excluded, log^{10}AFI was excluded from the range of accepted GLMs. Best GLMs (Table 5) included either MAR or SI. Explained deviance for all GLMs appeared to be particularly high for those in which rainfall seasonality index was used. Furthermore, due to collinearity (Table 3), seasonality index and mean annual rainfall were not used in the same GLM.

Table 5. Best models (ΔAIC = 0) for percentage of resprouting plants with the resprouting traits: apical, epicormic, basal/collar and underground

Resprouting Trait	***Best Model***	***R^2***
Apical	Logit(Apical) = -3.87 + 0.76 MAR	0.43
Epicormic	Logit(Epicormic) = -1.84 + 0.76 SI + 0.74 SI	0.91
Basal/Collar	Logit(Basal/Collar) = +1.2 + 0.97 SI	0.76
Underground	Logit(Underground) = -0.7 + 0.46 MAR	0.52

4.2.1 Apical Resprouters

The best GLM for apical resprouters contained just MAR (Figure 5) showing a positive relationship with an explained deviance of (R^2 = 0.43). Among the other candidate GLMs (Table 6), all other single variables were included, however, none had higher explained deviance. A full list of the GLMs is can be found in Appendix 3.

Table 6. Best GLMs (ΔAIC<2) for percentage of resprouters displaying apical resprouting traits

Predictor Variables										
x1	***x2***	***x3***	***x4***	***Coef Intercept***	***Coef x1***	***Coef x2***	***Coef x3***	***Coef x4***	***ΔAIC***	***R2 Dev***
MAR	/	/	/	-3.87	0.76	/	/	/	0.00	0.43
Tdry	/	/	/	-3.76	0.63	/	/	/	0.58	0.30
SI	/	/	/	-3.74	0.56	/	/	/	0.74	0.27
GD	/	/	/	-3.72	0.53	/	/	/	0.87	0.24
Pdry	/	/	/	-3.72	-0.57	/	/	/	0.94	0.23
PET	/	/	/	-3.66	0.43	/	/	/	1.40	0.13
MOB	/	/	/	-3.61	0.25	/	/	/	1.82	0.04
FRP	/	/	/	-3.60	-0.26	/	/	/	1.88	0.03
MAR	MAR	/	/	-3.95	0.66	0.10	/	/	1.97	0.43
FSC	/	/	/	-3.58	-0.08	/	/	/	1.98	0.00

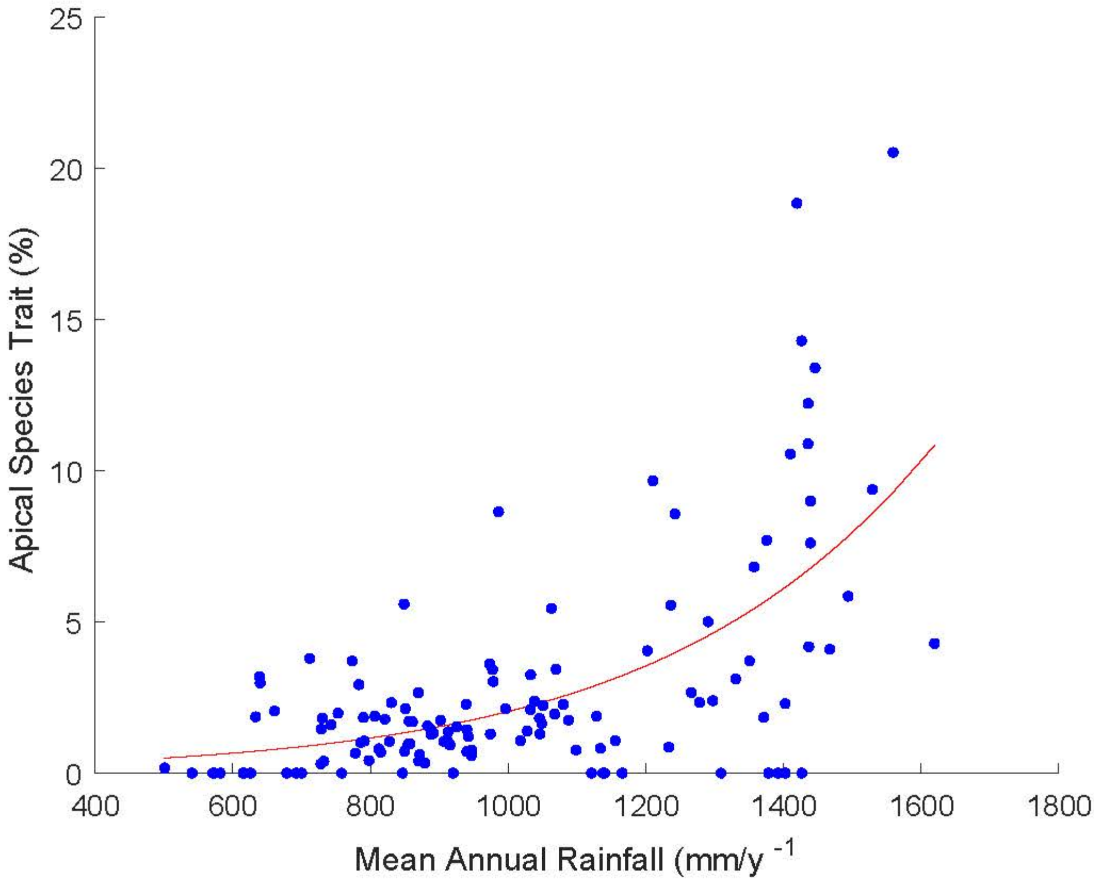

Figure 5. Percentage of resprouters with the apical resprouting trait as a function of mean annual rainfall (mm/y^{-1}) , red line indicating best model fit

4.2.2 Epicormic Resprouters

Best models (Table 7) regarding the epicormic resprouting trait all included either SI or GD. The best model contained SI through a parabolic fit, explaining 91% of deviance. What can be observed from Figure 6 is that there appears to be grouping of the variables predominantly in SI ranges 0.5-0.7 and 0.95-1.1 with little in between which may be explained by large spatial differences. A complete list of GLMs can be found in Appendix 4.

Table 7. Best GLMs (ΔAIC<2) for percentage of resprouters displaying epicormic resprouting traits

Predictor Variables										
x1	***x2***	***x3***	***x4***	***Coef Intercept***	***Coef x1***	***Coef x2***	***Coef x3***	***Coef x4***	***ΔAIC***	***R2 Dev***
SI	SI	/	/	-1.84	0.76	0.75	/	/	0.00	0.91
SI	/	/	/	-1.14	1.44	/	/	/	0.48	0.86
GD	GD	/	/	-1.80	0.74	0.73	/	/	1.28	0.88

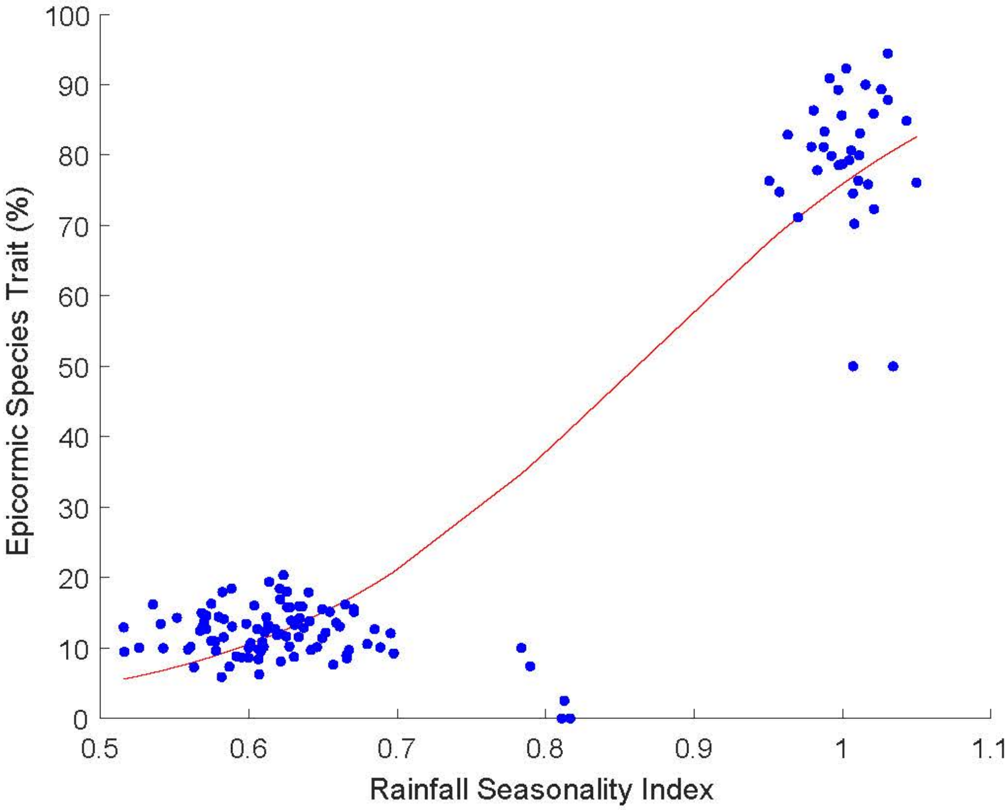

Figure 6. Percentage of resprouters displaying the epicormic resprouting trait as a function of rainfall seasonality index, red line indicating best model fit

4.2.3 Basal/Collar Resprouters

The best GLMs using basal/collar resprouters as a dependent variable was SI which identified a positive relationship, explaining 76% of deviance (Figure 7). Other potential GLMs (Table 8) included GD, Tdry, SI and potential evapotranspiration (PET) all of which explained similar amounts of deviance.

Table 8. Best GLMs (ΔAIC<2) for percentage of resprouters displaying basal/collar resprouting traits

Predictor Variables										
x1	***x2***	***x3***	***x4***	***Coef Intercept***	***Coef x1***	***Coef x2***	***Coef x3***	***Coef x4***	***ΔAIC***	***R2 Dev***
SI	/	/	/	1.20	0.97	/	/	/	0.00	0.76
GD	/	/	/	1.18	0.94	/	/	/	0.50	0.74
Tdry	/	/	/	1.18	0.89	/	/	/	0.52	0.74
Tdry	Tdry	/	/	0.94	0.81	0.28	/	/	1.83	0.77
SI	SI	/	/	1.07	0.89	0.14	/	/	1.88	0.77
PET	PET	/	/	0.90	0.94	0.32	/	/	1.92	0.77

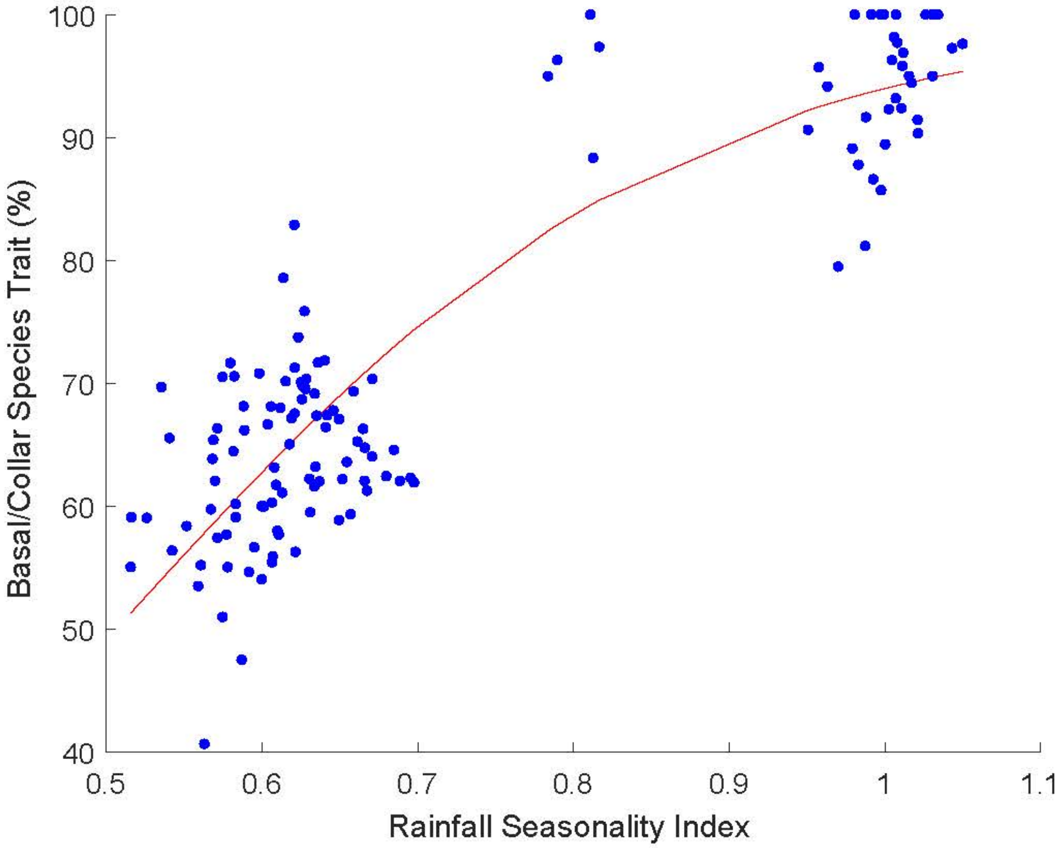

Figure 7. Percentage of resprouters displaying the basal/collar resprouting trait as a function of rainfall seasonality index, red line indicating best model fit

4.2.4 Underground Resprouting Trait

The best GLM for percentage of resprouters with the underground resprouting trait was with solely MAR (Figure 8), showing a positive relationship and explaining 52% of deviance. Other variables in the potential GLMs included SI & GD. Inclusion of GD in the GLM with MAR only resulted in a minor increase in explained deviance (R^2 = 0.56)

Table 9. Best GLMs (ΔAIC<2) for percentage of resprouters displaying underground resprouting traits

Predictor Variables										
x1	***x2***	***x3***	***x4***	***Coef Intercept***	***Coef x1***	***Coef x2***	***Coef x3***	***Coef x4***	***ΔAIC***	***R2 Dev***
MAR	/	/	/	-0.70	0.46	/	/	/	0.00	0.52
SI	/	/	/	-0.69	0.43	0.00	/	/	0.27	0.49
GD	GD	/	/	-1.14	0.02	0.44	/	/	0.93	0.61
GD	/	/	/	-0.69	0.40	/	/	/	1.06	0.42
GD	MAR	/	/	-0.70	0.18	0.33	/	/	1.52	0.56
SI	SI	/	/	-1.01	0.16	0.31	/	/	1.55	0.55
MAR	MAR	/	/	-0.73	0.44	0.03	/	/	1.97	0.52

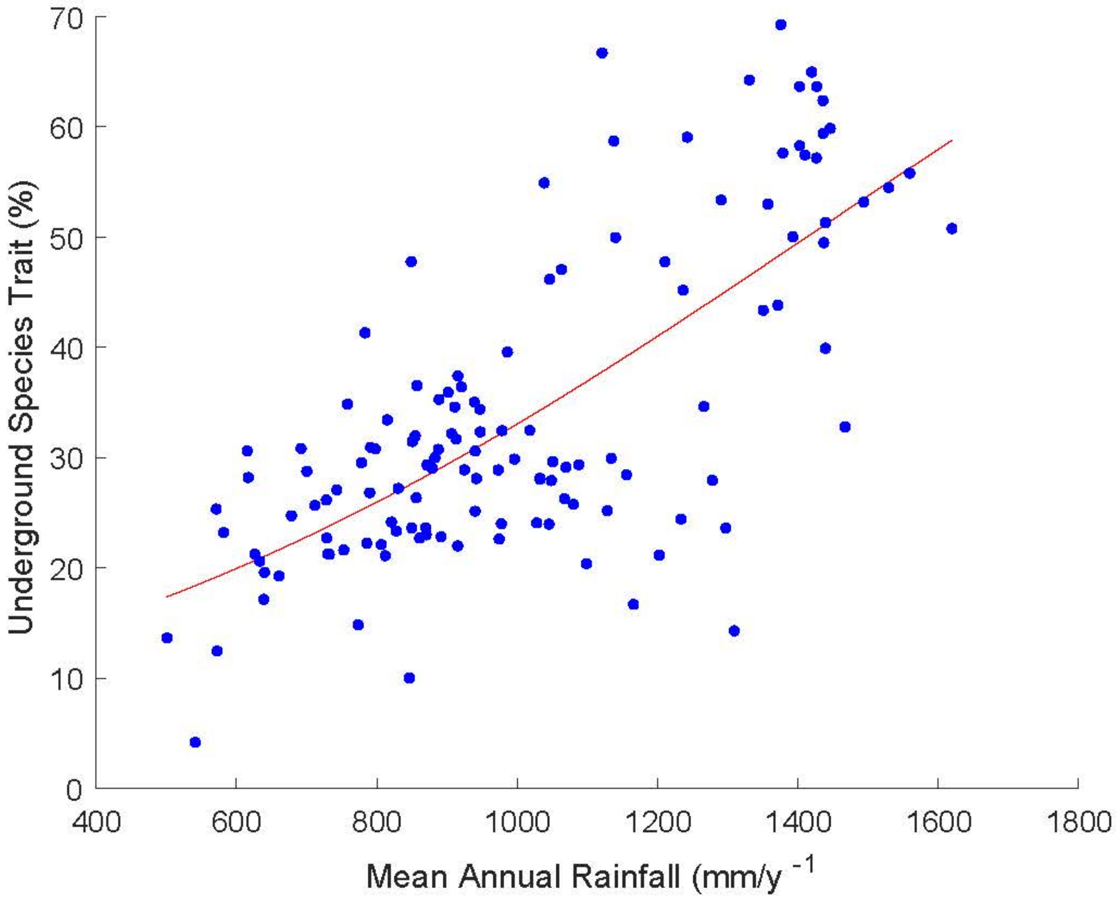

Figure 8. Percentage of resprouters displaying the underground resprouting trait as a function of mean annual rainfall (mm/y^{-1}), red line indicating best model fit

5 Discussion

5.1 What are the main determinants of the prevalence of resprouting taxa within plant communities?

Regarding the general percentage of resprouters relative to present species (RSpPer), MAR proved to be the best predictor. Log^{10}AFI by itself and Log^{10}AFI alongside MAR were also presented in the suite of suitable models to explain relative resprouter richness. The Pearson's correlation coefficient identified a moderate degree of negative correlation between Log^{10}AFI and MAR (r = -0.68) this was determined as marginally below the critical value (>0.7 or < -0.7). The model that used both variables did however present the highest explained deviance (R^2 = 0.40). With regards to the literature, resprouters are commonly shown to be more prevalent in more productive and fire-prone conditions (Russel-Smith et al. 2012; Clarke et al. 2013;) and in modelling studies has been shown to be an important factor in maintaining productivity in fire prone areas (Kelley & Harrison, 2014). The results of this study are therefore in general agreement with the surrounding literature. The life-history trade-offs regarding reduced reproductivity and increased allocation to NSCs in resprouters relative to non-resprouters generally make them better suited to areas of high productivity and fire frequency (Clarke et al. 2010; Clarke et al. 2013; Zeppel et al. 2014).

5.2 What are the main determinants of resprouter type occurrence within plant communities?

The decision to exclude log^{10}AFI from acceptable GLMs was made due to the extremely low AIC values that it provided (Appendix 3-6). As a result of this and using a criterion of ΔAIC<2, log^{10}AFI appeared as the only acceptable variable in all the GLMs, this resulted in a lack of inference from the GLMs. Furthermore, log^{10}AFI had high collinearity with a number of variables including Tdry, Dry Months, rainfall seasonality index and growing days so its exclusion allowed for relationships to be analysed for these variables as well which are hypothesised to have an effect on resprouter trait distribution.

The apical resprouting trait was the least represented in the resprouting trait species percentages with a range of 0-20.5%. This is likely due to their relatively small representation amongst resprouters (Clarke et al. 2013). The analysis shows that, MAR was the main determinant of the distribution of apical resprouters highlighting that increased MAR results in more species with the apical trait within plant communities. The results fit in with the surrounding literature in that they are represented by a smaller species percentage in areas of higher rainfall (Figure 1), (Clarke et al. 2013).

Epicormic resprouters like apical resprouters are aerial but are more widely represented by species, explaining the percentage ranges of epicormic resprouter (0-95%). The GLM results indicated that rainfall seasonality index (SI) was the best fir for the model along with the basal/collar resprouters. Both GLMs showed a large deal of grouping due to the associated SI values likely due to the lack of a spatial gradient of seasonality index associated with the disparity in latitudes of the study sites. Inferences are therefore difficult to make for both epicormic and basal/collar resprouters.

MAR was in the best model for underground resprouters suggesting that in areas of increased MAR, underground resprouting is more common. Underground resprouters occur in a wide range of MAR (Clarke et al. 2013).

5.3 Limitations

The vegetation data was collected over a large spatial gradient with stark differences in latitude, the most northern site was located at 12.15^{o} S and the southernmost at 37.5^{o} S, resulting in a range of 25.35^{o}. Due to the nature of data collection a large degree of latitudinal separation exists, particularly between the northern sites and those of the Sydney Basin and southwestern Australia. This lack of data at intermediate sites results in a stark contrast in variables between the different areas and therefore a lack of a gradient from which geospatial differences can be derived. This is particularly highlighted in the results for epicormic and basal/collar resprouting traits (Figures 6 & 7). The best models for epicormic and basal/resprouter explained 91% and 76% of deviance respectively, yet from observation of the plots (Figures 6 & 7) a polarity in the explanatory values is obvious which is likely to have influenced the results. This highlights the need for a more holistic gradient of sampling or alternatively, separate analysis of individual areas.

Data collection of vegetation data took place over a number of years from a series of studies, due to this the decision was made to investigate spatial changes in resprouting vegetation as opposed to temporal. For this a climatology was derived from 1997-1999. Due to this, the climatology of each area is not precisely up to date with that of the vegetation, this may have an impact on the results of the GLMs as missing climate and particularly fire data in the years before vegetation sampling may have had a significant impact on species composition in some areas due to recent disturbance events such as drought or fire. Previous studies that involved sampling of vegetation in fire-prone ecosystems have used last fire interval as an indicator as opposed to average fire interval in assessing resprouter mortality, highlighting significant differences in lignotuber mortality at timescale ranges of 1-40 years (Enright et al. 2011). This implies that disturbance events at short timescales can have significant effects on community assemblages.

It is acknowledged that a number of variables influence community composition at much smaller scales than 0.25^{o}, geological, hydrological and topographical heterogeneity results in a mosaic of community compositions within each cell (Russel-Smith, Edwards & price, 2012). The study, however, aims to assess the interactions of vegetation with climate and fire at a much broader scale, deriving patterns across Australia in which effects of climate and fire are more apparent.

References

Adams, M. A. (2013). *Mega-fires, tipping points and ecosystem services: Managing forests and woodlands in an uncertain future* doi:https://doi.org/10.1016/j.foreco.2012.11.039

Akaike, H. (1974). A new look at the statistical model identification. *IEEE Transactions on Automatic Control, 19*(6), 716-723.

Allen, C. D., Macalady, A. K., Chenchouni, H., Bachelet, D., McDowell, N., Vennetier, M., . Hogg, E. T. (2010). A global overview of drought and heat-induced tree mortality reveals emerging climate change risks for forests. *Forest Ecology and Management, 259*(4), 660-684.

Andela, N., D.C. Morton, L. Giglio, and J.T. Randerson. 2019. Global Fire Atlas with Characteristics of Individual Fires, 2003-2016. ORNL DAAC, Oak Ridge, Tennessee, USA. https://doi.org/10.3334/ORNLDAAC/1642

Anderson, D. R., & Burnham, K. P. (2002). Avoiding pitfalls when using information-theoretic methods. *The Journal of Wildlife Management, 66*(3), 912-918. doi:10.2307/3803155

Anthony L. Westerling, Monica G. Turner, Erica A. H. Smithwick, William H. Romme, & Michael G. Ryan. (2011). Continued warming could transform greater yellowstone fire regimes by mid-21st century. *Proceedings of the National Academy of Sciences of the United States of America, 108*(32), 13165-13170. doi:10.1073/pnas.1110199108

Archibald, S., Lehmann, C. E., Gómez-Dans, J. L., & Bradstock, R. A. (2013). Defining pyromes and global syndromes of fire regimes. *Proceedings of the National Academy of Sciences*, *110*(16), 6442-6447.

Baudena, M., Santana, V. M., Baeza, M. J., Bautista, S., Eppinga, M. B., Hemerik, L., Vallejo, V. R. (2020). Increased aridity drives postâ€fire recovery of mediterranean forests towards open shrublands. *New Phytologist, 225*(4), 1500-1515.

Bistinas, I., Harrison, S. P., Prentice, I. C., & Pereira, J. (2014). Causal relationships vs. emergent patterns in the global controls of fire frequency. *Biogeosciences, 11*, 5087-5101.

Boer, M. M., de Dios, V. R., & Bradstock, R. A. (2020). Unprecedented burn area of australian mega forest fires. *Nature Climate Change, 10*(3), 171-172.

Boer, M. M., Resco De Dios, V., Stefaniak, E. Z., & Bradstock, R. A. (2019). A hydroclimatic model for the distribution of fire on earth. *Biogeosciences Discussions,* , 1-21.

Bond, W. J. (2016). Ancient grasslands at risk. *Science, 351*(6269), 120-122.

Booth, G. D. (1994). *Identifying proxy sets in multiple linear regression: An aid to better coefficient interpretation* US Department of Agriculture, Forest Service, Intermountain Research Station.

Bowman, D. M., Balch, J. K., Artaxo, P., Bond, W. J., Carlson, J. M., Cochrane, M. A., Harrison, S. P. (2009). Fire in the earth system. *Science, 324*(5926), 481-484.

Bradstock, R. A. (2010). A biogeographic model of fire regimes in australia: Current and future implications. *Global Ecology and Biogeography, 19*(2), 145-158. doi:10.1111/j.1466-8238.2009.00512.x

Bradstock, R. A., & Kenny, B. J. (2003). An application of plant functional types to fire management in a conservation reserve in southeastern Australia. *Journal of Vegetation Science, 14*(3), 345-354.

Bréda, N., & Badeau, V. (2008). Forest tree responses to extreme drought and some biotic events: Towards a selection according to hazard tolerance? *Comptes Rendus Geoscience, 340*(9-10), 651-662.

Clarke, P. J., Lawes, M. J., & Midgley, J. J. (2010). Resprouting as a key functional trait in woody plants—challenges to developing new organizing principles. *The New Phytologist, 188*(3), 651-654.

Clarke, P. J., Lawes, M. J., Midgley, J. J., Lamont, B. B., Ojeda, F., Burrows, G. E., Knox, K. J. E. (2013). Resprouting as a key functional trait: How buds, protection and resources drive persistence after fire. *New Phytologist, 197*(1), 19-35. doi:10.1111/nph.12001

D'Onofrio, D., von Hardenberg, J., & Baudena, M. (2018). Not only trees: Grasses determine african tropical biome distributions via water limitation and fire. *Global Ecology and Biogeography, 27*(6), 714-725.

D’Onofrio, D., Sweeney, L., von Hardenberg, J., & Baudena, M. (2019). Grass and tree cover responses to intra-seasonal rainfall variability vary along a rainfall gradient in African tropical grassy biomes. *Scientific reports*, *9*(1), 1-10.

Dormann, C. F., Elith, J., Bacher, S., Buchmann, C., Carl, G., Carré, G., . . . Lautenbach, S. (2013). Collinearity: A review of methods to deal with it and a simulation study evaluating their performance. *Ecography, 36*(1), 27-46. doi:10.1111/j.1600-0587.2012.07348.x

Dr. Tingbao Xu , Dr. Wang Han , Prof. Michael Hutchinson , Julie Pauwels , Dr. Rhys Whitley , Dr. Bradley Evans (2015): eMAST-R-Package collection. Version . Ecosystem Modelling and Scaling Infrastructure. dataset.

Edwards, A., Kennett, R., Price, O., Russell-Smith, J., Spiers, G., & Woinarski, J. (2003). Monitoring the impacts of fire regimes on vegetation in northern australia: An example from kakadu national park. *International Journal of Wildland Fire, 12*(4), 427-440.

Ell, K. 2020. Australia’s Bushfires: The Economic Costs. Moody’s Analytics. Accessed on June 12th, 2020 from: https://www.economy.com/economicview/analysis/377681

Enright, N. J., Fontaine, J. B., Westcott, V. C., Lade, J. C., & Miller, B. P. (2011). Fire interval effects on persistence of resprouter species in mediterranean-type shrublands. *Plant Ecology, 212*(12), 2071-2083.

Etchells, H., O'Donnell, A. J., Lachlan McCaw, W., & Grierson, P. F. (2020). *Fire severity impacts on tree mortality and post-fire recruitment in tall eucalypt forests of southwest Australia* doi:https://doi.org/10.1016/j.foreco.2019.117850

Gill, A. M. (1981). Adaptive responses of Australian vascular plant species to fires. *Fire and the Australian Biota*, 243-272.

Guisan, A., & Zimmermann, N. E. (2000). Predictive habitat distribution models in ecology. *Ecological Modelling, 135*(2), 147-186. doi:https://doi.org/10.1016/S0304-3800(00)00354-9

Guisan, A., Edwards, T. C., & Hastie, T. (2002). Generalized linear and generalized additive models in studies of species distributions: Setting the scene. *Ecological Modelling, 157*(2), 89-100. doi:https://doi.org/10.1016/S0304-3800(02)00204-1

Haverd, V., Raupach, M. R., Briggs, P. R., Davis, S. J., Law, R. M., Meyer, C. P., Sherman, B. (2013). The Australian terrestrial carbon budget.

Heimann, M., Esser, G., Haxeltine, A., Kaduk, J., Kicklighter, D. W., Knorr, W., . . . Moore Iii, B. (1998). Evaluation of terrestrial carbon cycle models through simulations of the seasonal cycle of atmospheric CO2: First results of a model intercomparison study. *Global Biogeochemical Cycles, 12*(1), 1-24. https://earthdata.nasa.gov/firms.

Karavani, A., Boer, M. M., Baudena, M., Colinas, C., Diaz-Sierra, R., Peman, J., Resco de Dios, V. (2018). Fire induced deforestation in drought prone Mediterranean forests: Drivers and unknowns from leaves to communities. *Ecological Monographs, 88*(2), 141-169.

Keeley, J. E., Bond, W. J., Bradstock, R. A., Pausas, J. G., & Rundel, P. W. (2011). *Fire in mediterranean ecosystems: Ecology, evolution and management* Cambridge University Press.

Kelley, D. I., & Harrison, S. P. (2014). Enhanced australian carbon sink despite increased wildfire during the 21st century. *Environmental Research Letters, 9*(10), 104015.

Kelley, D. I., Harrison, S. P., & Prentice, I. C. (2014). Improved simulation of fire vegetation interactions in the land surface processes and exchanges dynamic global vegetation model (LPX-Mv1). *Geoscientific Model Development, 7*(5), 2411-2433.

Kelley, D. I., Prentice, I. C., Harrison, S. P., Wang, H., Simard, M., Fisher, J. B., & Willis, K. O. (2013). A comprehensive benchmarking system for evaluating global vegetation models. *Biogeosciences, 10*(5), 3313-3340. doi:10.5194/bg-10-3313-2013

Lasslop, G., Brovkin, V., Reick, C. H., Bathiany, S., & Kloster, S. (2016). Multiple stable states of tree cover in a global land surface model due to a fire vegetation feedback. *Geophysical Research Letters, 43*(12), 6324-6331.

Lehmann, C. E. R., Archibald, S. A., Hoffmann, W. A., & Bond, W. J. (2011). Deciphering the distribution of the savanna biome. *New Phytologist, 191*(1), 197-209. doi:10.1111/j.1469-8137.2011.03689.x

Liu, Y., Stanturf, J., & Goodrick, S. (2010). *Trends in global wildfire potential in a changing climate* doi:https://doi.org/10.1016/j.foreco.2009.09.002

McArthur, A. G., & Luke, R. H. (1978). Bushfires in Australia. *Canberra, Australia: Australian Government Publishing Service,*

MODIS Collection 6 NRT Hotspot, 2020 Active Fire Detection MCD14ML. Accessed from https://earthdata.nasa.gov/firms. Accessed on 24/05/2020

Moritz, M. A., Batllori, E., Bradstock, R. A., Gill, A. M., Handmer, J., Hessburg, P. F., Schoennagel, T. (2014). Learning to coexist with wildfire. *Nature, 515*(7525), 58-66.

Moritz, M. A., Parisien, M., Batllori, E., Krawchuk, M. A., Van Dorn, J., Ganz, D. J., & Hayhoe, K. (2012). Climate change and disruptions to global fire activity. *Ecosphere, 3*(6), 1-22.

Pausas, J. G., & Bradstock, R. A. (2007). Fire persistence traits of plants along a productivity and disturbance gradient in mediterranean shrublands of southeast Australia. *Global Ecology and Biogeography, 16*(3), 330-340.

Pausas, J. G., & Ribeiro, E. (2013). The global fire productivity relationship. *Global Ecology and Biogeography, 22*(6), 728-736.

Pausas, J. G., Pratt, R. B., Keeley, J. E., Jacobsen, A. L., Ramirez, A. R., Vilagrosa, A., Davis, S. D. (2016). Towards understanding resprouting at the global scale. *New Phytologist, 209*(3), 945-954.

Pekin, B. K., Wittkuhn, R. S., Boer, M. M., Macfarlane, C., & Grierson, P. F. (2011). Plant functional traits along environmental gradients in seasonally dry and fire-prone ecosystem. *Journal of Vegetation Science, 22*(6), 1009-1020.

Randerson, J.T., G.R. van der Werf, L. Giglio, G.J. Collatz, and P.S. Kasibhatla. 2018. Global Fire Emissions Database, Version 4.1 (GFEDv4). ORNL DAAC, Oak Ridge, Tennessee, USA. https://doi.org/10.3334/ORNLDAAC/1293

Russell-Smith, J., Edwards, A. C., & Price, O. F. (2012). Simplifying the savanna: The trajectory of fire-sensitive vegetation mosaics in northern australia. *Journal of Biogeography, 39*(7), 1303-1317. doi:10.1111/j.1365-2699.2012.02679.x

Russell-Smith, J., Gardener, M. R., Brock, C., Brennan, K., Yates, C. P., & Grace, B. (2012). Fire persistence traits can be used to predict vegetation response to changing fire regimes at expansive landscape scales an Australian example. *Journal of Biogeography, 39*(9), 1657-1668.

Russell-Smith, J., Yates, C. P., Whitehead, P. J., Smith, R., Craig, R., Allan, G. E., . . . Meyer, M. C. (2007). Bushfires ‘down under’: Patterns and implications of contemporary australian landscape burning. *International Journal of Wildland Fire, 16*(4), 361-377.

Staver, A. C., Archibald, S., & Levin, S. (2011). Tree cover in subâ€Saharan africa: Rainfall and fire constrain forest and savanna as alternative stable states. *Ecology, 92*(5), 1063-1072.

Staver, A. C., Bond, W. J., Stock, W. D., Van Rensburg, S. J., & Waldram, M. S. (2009). Browsing and fire interact to suppress tree density in an african savanna. *Ecological Applications, 19*(7), 1909-1919.

Stern, H., De Hoedt, G., & Ernst, J. (2000). Objective classification of Australian climates. *Australian Meteorological Magazine, 49*(2), 87-96.

Stevens-Rumann, C., Kemp, K. B., Higuera, P. E., Harvey, B. J., Rother, M. T., Donato, D. C., Veblen, T. T. (2018). Evidence for declining forest resilience to wildfires under climate change. *Ecology Letters, 21*(2), 243-252. doi:10.1111/ele.12889

TERN AusCover. (2016). Australian Gridded Climate Data. Obtained from auscover.org.au/datasets/australian-gridded-climate-data/#:~:text=Browse All Data-,Australian Gridded Climate Data,at daily and monthly timescales, Accessed 22/05/2020

Walsh, R., & Lawler, D. M. (1981). Rainfall seasonality: Description, spatial patterns and change through time. *Weather, 36*(7), 201-208.

Wang, L., Hunt Jr, E. R., Qu, J. J., Hao, X., & Daughtry, C. S. (2013). Remote sensing of fuel moisture content from ratios of narrow-band vegetation water and dry-matter indices. *Remote Sensing of Environment, 129*, 103-110.

Williams, R. J., Gill, A. M., & Bradstock, R. A. (2012). *Flammable australia: Fire regimes, biodiversity and ecosystems in a changing world* CSIRO publishing.

Yue, C., Ciais, P., Zhu, D., Wang, T., Peng, S., & Piao, L. (2016). How have past fire disturbances contributed to the current carbon balance of boreal ecosystems? *Biogeosciences Discussions, 13*, 675

Zeppel, M. J., Harrison, S. P., Adams, H. D., Kelley, D. I., Li, G., Tissue, D. T., . . . Palmer, A. (2015). Drought and resprouting plants. *New Phytologist, 206*(2), 583-589.

Appendices

	MAR	TMax	Pdry	Pwet	Tdry	Twet	DM	SI	RR	RCPer	RSpPer	BA	LogAFI	AFI	MOB	FSC
MAR	1.00	0.73	-0.42	0.97	0.60	0.70	0.76	0.70	-0.38	0.22	0.17	0.11	0.05	-0.01	-0.07	-0.13
TMax	0.73	1.00	-0.87	0.84	0.93	0.94	0.94	0.96	-0.67	0.36	0.33	0.30	0.26	0.23	0.20	0.16
Pdry	-0.42	-0.87	1.00	-0.59	-0.88	-0.78	-0.82	-0.90	0.72	-0.34	-0.33	-0.32	-0.30	-0.29	-0.28	-0.27
Pwet	0.97	0.84	-0.59	1.00	0.69	0.81	0.87	0.82	-0.53	0.26	0.21	0.15	0.10	0.04	-0.01	-0.07
Tdry	0.60	0.93	-0.88	0.69	1.00	0.77	0.85	0.94	-0.60	0.37	0.35	0.33	0.31	0.29	0.27	0.25
Twet	0.70	0.94	-0.78	0.81	0.77	1.00	0.89	0.83	-0.67	0.31	0.27	0.23	0.20	0.16	0.12	0.08
DM	0.76	0.94	-0.82	0.87	0.85	0.89	1.00	0.95	-0.76	0.32	0.28	0.24	0.20	0.16	0.12	0.08
SI	0.70	0.96	-0.90	0.82	0.94	0.83	0.95	1.00	-0.71	0.36	0.33	0.30	0.27	0.24	0.21	0.18
RR	-0.38	-0.67	0.72	-0.53	-0.60	-0.67	-0.76	-0.71	1.00	-0.10	-0.06	-0.02	0.02	0.06	0.10	0.14
RCPer	0.58	0.35	-0.14	0.55	0.25	0.33	0.40	0.36	-0.05	0.16	0.13	0.11	0.08	0.05	0.03	0.00
RSpPer	0.60	0.42	-0.16	0.59	0.31	0.42	0.41	0.39	-0.03	0.19	0.17	0.14	0.11	0.08	0.06	0.03
BA	0.66	0.84	-0.68	0.77	0.71	0.82	0.87	0.82	-0.64	0.29	0.25	0.22	0.18	0.15	0.11	0.08
LogAFI	-0.68	-0.76	0.54	-0.71	-0.67	-0.73	-0.72	-0.71	0.31	-0.33	-0.30	-0.27	-0.25	-0.22	-0.19	-0.17
AFI	-0.28	-0.31	0.20	-0.27	-0.32	-0.30	-0.23	-0.27	0.00	-0.17	-0.16	-0.15	-0.15	-0.14	-0.13	-0.13
MOB	0.62	0.55	-0.29	0.63	0.38	0.61	0.59	0.46	-0.29	0.18	0.15	0.11	0.07	0.04	0.00	-0.04
FSC	0.31	0.08	0.16	0.24	-0.09	0.21	0.08	-0.04	0.17	0.03	0.01	-0.01	-0.02	-0.04	-0.06	-0.08

Appendix 1 – Pearson's correlation coefficient for all variables

Predictor Variables										
x1	x2	x3	x4	Coef Intercept	Coef x1	Coef x2	Coef x3	Coef x4	∆AIC	R^2 Deviance
MAR	/	/	/	1.40	0.44	/	/	/	0.00	0.340
log^{10}AFI	/	/	/	1.38	-0.31	/	/	/	1.67	0.183
log^{10}AFI	log^{10}AFI^2	/	/	1.38	-0.31	/	/	/	1.67	0.183
RS	/	/	/	1.38	0.32	/	/	/	1.73	0.178
DM	/	/	/	1.38	0.31	/	/	/	1.93	0.159
MAR	log^{10}AFI	/	/	1.40	0.39	-0.07	/	/	1.93	0.399
MAR	MAR^2	/	/	1.44	0.44	-0.04	/	/	1.96	0.343
MAR	PET	/	/	1.40	0.44	-0.01	/	/	2.00	0.387
MAR	GD	/	/	1.40	0.43	0.01	/	/	2.00	0.386
MAR	TDry	/	/	1.40	0.44	-0.01	/	/	2.00	0.386
GD	/	/	/	1.37	0.29	/	/	/	2.03	0.149
TDry	/	/	/	1.36	0.22	/	/	/	2.69	0.088
MOB	/	/	/	1.36	0.19	/	/	/	2.78	0.079
PET	/	/	/	1.36	0.16	/	/	/	3.07	0.052
PDry	/	/	/	1.35	-0.10	/	/	/	3.40	0.021
FSC	/	/	/	1.35	0.05	/	/	/	3.56	0.006
log^{10}AFI	PET	/	/	1.38	-0.33	-0.04	/	/	3.65	0.214
log^{10}AFI	FSC	/	/	1.38	-0.31	-0.02	/	/	3.66	0.211
GD	GD^2	/	/	1.19	0.14	0.19	/	/	3.70	0.180
RS	RS^2	/	/	1.38	-0.02	0.34	/	/	3.72	0.191
DM	DM^2	/	/	1.64	0.61	-0.26	/	/	3.74	0.177
MOB	GD	/	/	1.38	0.11	0.25	/	/	3.80	0.180
PET	PET^2	/	/	1.21	0.20	0.17	/	/	3.82	0.169
PDry	PDry^2	/	/	1.05	-0.04	0.33	/	/	3.82	0.169
MAR	log^{10}AFI	PET	/	1.40	0.39	-0.10	-0.06	/	3.89	0.405
MAR	log^{10}AFI	TDry	/	1.40	0.40	-0.10	-0.05	/	3.90	0.403
MAR	log^{10}AFI	RS	/	1.41	0.39	-0.08	-0.03	/	3.91	0.402
MAR	MAR^2	MAR^3	/	1.44	0.44	-0.04	0.00	/	3.96	0.343
MOB	MOB^2	/	/	1.25	0.32	0.12	/	/	4.29	0.125
PDry	PDry^2	PDry^3	/	0.77	0.73	0.54	-0.42	/	4.42	0.300
TDry	TDry^2	/	/	1.20	0.13	0.17	/	/	4.44	0.111
MOB	PET	/	/	1.36	0.16	0.12	/	/	4.52	0.103
MOB	FS	/	/	1.36	0.21	-0.03	/	/	4.76	0.088
DM	DM^2	DM3	/	1.07	0.43	0.81	-0.42	/	5.40	0.208
TDry	TDry^2	TDry3	/	1.01	-0.60	0.13	0.47	/	5.49	0.200
FS	FS^2	/	/	1.32	0.09	0.03	/	/	5.53	0.009
PET	PET^2	PET^3	/	1.11	-0.01	0.28	0.07	/	5.64	0.186
log^{10}AFI	FSC	TDry	/	1.38	-0.34	-0.04	-0.03	/	5.65	0.213
log^{10}AFI	log^{10}AFI^2	log^{10}AFI^3	/	1.38	-0.31	0.00	0.00	/	5.67	0.183
RS	RS^2	RS^3	/	1.41	0.52	0.08	-0.13	/	5.67	0.183
GD	GD^2	GD^3	/	1.16	0.00	0.15	0.08	/	5.68	0.182
MAR	log^{10}AFI	FS	TDry	1.40	0.42	-0.18	-0.11	-0.15	5.77	0.422
MAR	log^{10}AFI	TDry	MOB	1.40	0.43	-0.16	-0.10	-0.08	5.84	0.411

MOB	MOB^2	MOB^3	/	1.32	0.47	-0.03	-0.09	/	6.02	0.150
FSC	FSC^2	FSC^3	/	1.39	0.24	-0.13	-0.08	/	7.25	0.035

Appendix 2 – GLMs for resprouter species percentage (%) using predictor variables: mean annual rainfall (MAR), precipitation in the driest month (PDry), temperature in the driest month (TDry), dry months (DM), seasonality index (SI), potential evapotranspiration (PET), growing days (GD), log^{10} average fire interval, months of burn (MOB), fires seasonal concentration (FSC) . ∆AIC indicates the AIC values relative to the value of the best GLM, explained deviance is explained through the R^2 Deviance.

Predictor Variables				Apical						
x1	x2	x3	x4	Coef Intercept	Coef x1	Coef x2	Coef x3	Coef x4	AIC Diff	R2 Dev
logAFI				-2.20	-0.58	0.00	0.00	0.00	0.00	0.16
logAFI	TDry			-5.10	0.53	1.06	0.00	0.00	1.16	0.39
logAFI	MAR			-4.08	0.08	0.76	0.00	0.00	1.18	0.38
logAFI	GD			-4.68	0.36	0.79	0.00	0.00	1.51	0.29
logAFI	RS			-4.06	0.14	0.60	0.00	0.00	1.71	0.24
logAFI	logAFI			-2.60	-0.19	-0.08	0.00	0.00	1.99	0.17
MAR				-3.87	0.76	0.00	0.00	0.00	2.24	0.43
Tdry				-3.76	0.63	0.00	0.00	0.00	2.83	0.30
logAFI	MAR	Tdry		-5.61	0.70	0.52	0.74	0.00	2.87	0.46
RS				-3.74	0.56	0.00	0.00	0.00	2.99	0.27
logAFI	MAR	GD		-5.02	0.45	0.64	0.38	0.00	3.09	0.41
GD				-3.72	0.53	0.00	0.00	0.00	3.12	0.24
logAFI	MAR	RS		-4.63	0.30	0.70	0.23	0.00	3.14	0.39
Pdry				-3.72	-0.57	0.00	0.00	0.00	3.18	0.23
logAFI	GD	RS		-4.56	0.30	1.20	-0.45	0.00	3.48	0.30
PET				-3.66	0.43	0.00	0.00	0.00	3.64	0.13
MOB				-3.61	0.25	0.00	0.00	0.00	4.06	0.04
FRP				-3.60	-0.26	0.00	0.00	0.00	4.12	0.03
MAR	MAR			-3.95	0.66	0.10	0.00	0.00	4.21	0.43
FSC				-3.58	-0.08	0.00	0.00	0.00	4.23	0.00
RS	MAR			-3.86	0.06	0.71	0.00	0.00	4.24	0.43
GD	MAR			-3.86	0.01	0.75	0.00	0.00	4.24	0.43
Tdry	Tdry			-3.66	0.71	-0.11	0.00	0.00	4.82	0.30
RS	TDry			-3.76	0.11	0.53	0.00	0.00	4.82	0.30
GD	TDry			-3.76	0.01	0.62	0.00	0.00	4.83	0.30
RS	RS			-3.54	0.78	-0.22	0.00	0.00	4.95	0.28
RS	GD			-3.74	0.54	0.02	0.00	0.00	4.99	0.27
Pdry	Pdry			-4.04	-0.44	0.30	0.00	0.00	5.02	0.26
GD	GD			-3.96	0.30	0.24	0.00	0.00	5.06	0.25
logAFI	GD	RS	Tdry	-4.77	0.41	-0.30	-0.21	0.00	5.09	0.40
PET	PET			-3.97	0.39	0.25	0.00	0.00	5.14	0.23
MOB	MOB			-3.92	0.43	0.27	0.00	0.00	5.67	0.12
FRP	FRP			-3.63	-0.34	0.03	0.00	0.00	6.10	0.03
FSC	FSC			-3.55	-0.11	-0.03	0.00	0.00	6.22	0.01

Appendix 2 – GLMs for percentage of resprouters that are apical, using predictor variables: mean annual rainfall (MAR), precipitation in the driest month (PDry), temperature in the driest month (TDry), dry months (DM), seasonality index (SI), potential evapotranspiration (PET), growing days (GD), $\log^{10}$ average fire interval, months of burn (MOB), fires seasonal concentration (FSC) and fire radiative power (FRP) . ∆AIC indicates the AIC values relative to the value of the best GLM, explained deviance is explained through the R^2 Deviance.

Predictor Variables				Epicormic						
x1	x2	x3	x4	Coef Intercept	Coef x1	Coef x2	Coef x3	Coef x4	AIC Diff	R2 Dev
logAFI	GD			-0.69	-0.17	1.35	0.00	0.00	0.00	0.93
logAFI	RS			-0.34	-0.27	1.27	0.00	0.00	0.10	0.93
logAFI	GD	RS		-0.74	-0.13	0.74	0.65	0.00	1.60	0.94
logAFI	TDry			0.06	-0.42	1.25	0.00	0.00	1.79	0.89
logAFI	MAR	GD		-0.71	-0.16	0.04	1.32	0.00	1.99	0.93
logAFI	MAR	RS		-0.37	-0.26	0.06	1.24	0.00	2.09	0.93
logAFI	GD	RS	Tdry	-0.75	-0.12	0.60	0.66	0.00	3.58	0.94
logAFI	logAFI			8.68	-6.74	1.05	0.00	0.00	3.65	0.86
logAFI	MAR	Tdry		-0.04	-0.39	0.14	1.17	0.00	3.68	0.90
logAFI	MAR			2.26	-1.37	0.55	0.00	0.00	5.99	0.81
logAFI				3.49	-1.84	0.00	0.00	0.00	6.64	0.75
RS	RS			-1.84	0.76	0.75	0.00	0.00	10.95	0.91
RS				-1.14	1.44	0.00	0.00	0.00	11.43	0.86
RS	MAR			-1.15	1.16	0.40	0.00	0.00	11.87	0.89
GD	GD			-1.80	0.74	0.73	0.00	0.00	12.23	0.88
RS	GD			-1.13	1.04	0.43	0.00	0.00	12.88	0.87
RS	TDry			-1.14	1.68	-0.26	0.00	0.00	13.19	0.87
GD	MAR			-1.13	1.07	0.50	0.00	0.00	13.30	0.86
PET	PET			-1.65	1.22	0.54	0.00	0.00	13.65	0.86
GD				-1.12	1.41	0.00	0.00	0.00	13.68	0.82
GD	TDry			-1.12	1.36	0.06	0.00	0.00	15.67	0.82
Pdry	Pdry			-1.83	-1.04	0.72	0.00	0.00	18.90	0.77
Tdry				-1.11	1.29	0.00	0.00	0.00	21.70	0.68
Pdry				-1.15	-1.33	0.00	0.00	0.00	22.80	0.66
PET				-1.15	1.39	0.00	0.00	0.00	23.22	0.65
Tdry	Tdry			-1.34	1.11	0.26	0.00	0.00	23.32	0.69
MAR				-1.14	1.30	0.00	0.00	0.00	24.45	0.63
MAR	MAR			-1.26	1.18	0.17	0.00	0.00	26.03	0.64
MOB	MOB			-1.41	1.03	0.43	0.00	0.00	44.23	0.32
MOB				-0.99	0.81	0.00	0.00	0.00	47.95	0.22
FSC	FSC			-0.60	-0.32	-0.29	0.00	0.00	58.85	0.06
FRP				-0.86	-0.19	0.00	0.00	0.00	59.49	0.01
FSC				-0.85	0.00	0.00	0.00	0.00	60.21	0.00
FRP	FRP			-0.85	-0.15	-0.01	0.00	0.00	61.46	0.01

Appendix 3 – GLMs for percentage of resprouters that are epicormic, using predictor variables: mean annual rainfall (MAR), precipitation in the driest month (PDry), temperature in the driest month (TDry), dry months (DM), seasonality index (SI), potential evapotranspiration (PET), growing days (GD), $\log^{10}$ average fire interval, months of burn (MOB), fires seasonal concentration (FSC) and fire radiative power (FRP) . ΔAIC indicates the AIC values relative to the value of the best GLM, explained deviance is explained through the R^2 Deviance.

Predictor Variables				Basal/Collar						
x1	x2	x3	x4	Coef Intercept	Coef x1	Coef x2	Coef x3	Coef x4	AIC Diff	R2 Dev
logAFI	GD			1.31	-0.07	0.88	0.00	0.00	0.00	0.81
logAFI	RS			1.56	-0.15	0.86	0.00	0.00	0.07	0.81
logAFI	logAFI			8.13	-5.00	0.81	0.00	0.00	0.65	0.77
logAFI	TDry			1.76	-0.23	0.73	0.00	0.00	1.38	0.72
logAFI	GD	RS		1.31	-0.05	0.50	0.45	0.00	1.67	0.83
logAFI	MAR	GD		1.30	-0.07	0.01	0.87	0.00	2.00	0.81
logAFI	MAR	RS		1.63	-0.17	-0.09	0.91	0.00	2.01	0.81
logAFI				3.14	-0.83	0.00	0.00	0.00	2.46	0.53
logAFI	MAR	Tdry		1.68	-0.21	0.08	0.70	0.00	3.33	0.73
logAFI	GD	RS	Tdry	1.31	-0.06	0.51	0.45	0.00	3.67	0.83
logAFI	MAR			2.60	-0.62	0.27	0.00	0.00	3.82	0.57
RS				1.20	0.97	0.00	0.00	0.00	14.00	0.76
GD				1.18	0.94	0.00	0.00	0.00	14.49	0.74
Tdry				1.18	0.89	0.00	0.00	0.00	14.52	0.74
RS	TDry			1.22	0.60	0.42	0.00	0.00	15.20	0.80
RS	GD			1.22	0.58	0.46	0.00	0.00	15.40	0.79
GD	TDry			1.20	0.53	0.45	0.00	0.00	15.59	0.78
RS	MAR			1.20	1.07	-0.13	0.00	0.00	15.82	0.77
Tdry	Tdry			0.94	0.81	0.28	0.00	0.00	15.82	0.77
RS	RS			1.07	0.89	0.14	0.00	0.00	15.88	0.77
PET	PET			0.90	0.94	0.32	0.00	0.00	15.92	0.77
Pdry	Pdry			0.77	-0.79	0.43	0.00	0.00	16.01	0.76
GD	GD			1.08	0.88	0.13	0.00	0.00	16.35	0.75
GD	MAR			1.18	0.94	0.00	0.00	0.00	16.49	0.74
Pdry				1.11	-0.73	0.00	0.00	0.00	17.32	0.59
PET				1.07	0.66	0.00	0.00	0.00	19.02	0.50
MAR	MAR			0.76	0.46	0.33	0.00	0.00	23.41	0.38
MAR				1.03	0.48	0.00	0.00	0.00	23.63	0.27
MOB	MOB			0.64	0.49	0.40	0.00	0.00	25.13	0.29
FSC				0.99	-0.18	0.00	0.00	0.00	28.06	0.04
MOB				0.99	0.14	0.00	0.00	0.00	28.29	0.03
FRP				0.98	-0.07	0.00	0.00	0.00	28.71	0.01
FSC	FSC			0.97	-0.16	0.02	0.00	0.00	30.04	0.04
FRP	FRP			0.99	-0.04	-0.01	0.00	0.00	30.69	0.01

Appendix 4 – GLMs for percentage of resprouters that are basal/collar, using predictor variables: mean annual rainfall (MAR), precipitation in the driest month (PDry), temperature in the driest month (TDry), dry months (DM), seasonality index (SI), potential evapotranspiration (PET), growing days (GD), log^{10} average fire interval, months of burn (MOB), fires seasonal concentration (FSC) and fire radiative power (FRP) . ∆AIC indicates the AIC values relative to the value of the best GLM, explained deviance is explained through the R^2 Deviance.

Predictor Variables										
x1	**x2**	**x3**	**x4**	**Coef Intercept**	**Coef x1**	**Coef x2**	**Coef x3**	**Coef x4**	**AIC Diff**	**R2 Dev**
logAFI				0.63	-0.52	0.00	0.00	0.00	0.00	0.46
logAFI	**RS**			-0.58	-0.04	0.43	0.00	0.00	0.49	0.63
logAFI	**TDry**			-0.47	-0.07	0.44	0.00	0.00	0.69	0.60
logAFI	**GD**			-0.55	-0.06	0.41	0.00	0.00	0.76	0.60
logAFI	**MAR**			0.02	-0.29	0.27	0.00	0.00	1.14	0.55
logAFI	**logAFI**			2.11	-1.90	0.29	0.00	0.00	1.35	0.53
logAFI	**MAR**	**RS**		-0.67	-0.01	0.13	0.36	0.00	2.34	0.64
logAFI	**MAR**	**Tdry**		-0.60	-0.03	0.15	0.35	0.00	2.47	0.63
logAFI	**GD**	**RS**		-0.60	-0.03	0.04	0.40	0.00	2.49	0.63
logAFI	**MAR**	**GD**		-0.65	-0.02	0.16	0.32	0.00	2.54	0.62
logAFI	**GD**	**RS**	**Tdry**	-0.64	-0.01	-0.21	0.41	0.00	4.35	0.64
MAR				-0.70	0.46	0.00	0.00	0.00	16.25	0.52
RS				-0.69	0.43	0.00	0.00	0.00	16.52	0.49
GD	**GD**			-1.14	0.02	0.44	0.00	0.00	17.19	0.61
GD				-0.69	0.40	0.00	0.00	0.00	17.31	0.42
RS	**MAR**			-0.70	0.24	0.28	0.00	0.00	17.47	0.58
GD	**MAR**			-0.70	0.18	0.33	0.00	0.00	17.77	0.56
RS	**RS**			-1.01	0.16	0.31	0.00	0.00	17.80	0.55
MAR	**MAR**			-0.73	0.44	0.03	0.00	0.00	18.22	0.52
RS	**TDry**			-0.70	0.65	-0.24	0.00	0.00	18.23	0.52
Tdry				-0.68	0.35	0.00	0.00	0.00	18.47	0.32
RS	**GD**			-0.69	0.45	-0.02	0.00	0.00	18.52	0.49
PET	**PET**			-0.87	0.34	0.18	0.00	0.00	18.81	0.47
Pdry				-0.68	-0.34	0.00	0.00	0.00	18.85	0.29
PET				-0.68	0.34	0.00	0.00	0.00	18.86	0.29
GD	**TDry**			-0.69	0.46	-0.07	0.00	0.00	19.29	0.42
Pdry	**Pdry**			-0.93	-0.28	0.25	0.00	0.00	19.64	0.39
Tdry	**Tdry**			-0.94	0.21	0.26	0.00	0.00	19.77	0.38
MOB				-0.68	0.25	0.00	0.00	0.00	20.51	0.14
FRP				-0.67	-0.06	0.00	0.00	0.00	22.04	0.01
FSC				-0.67	0.03	0.00	0.00	0.00	22.10	0.00
MOB	**MOB**			-0.77	0.31	0.09	0.00	0.00	22.18	0.17
FSC	**FSC**			-0.53	-0.14	-0.14	0.00	0.00	23.10	0.09
FRP	**FRP**			-0.68	-0.11	0.01	0.00	0.00	23.99	0.01

Appendix 6 – GLMs for percentage of resprouters that are underground, using predictor variables: mean annual rainfall (MAR), precipitation in the driest month (PDry), temperature in the driest month (TDry), dry months (DM), seasonality index (SI), potential evapotranspiration (PET), growing days (GD), $\log^{10}$ average fire interval, months of burn (MOB), fires seasonal concentration (FSC) and fire radiative power (FRP) . ∆AIC indicates the AIC values relative to the value of the best GLM, explained deviance is explained through the R^2 Deviance.